

PHYSICS IN COLLISION - Zeuthen, Germany, June 26-28, 2003

TOP AND ELECTROWEAK PHYSICS FROM THE TEVATRON

Mark C. Kruse

(Representing the CDF and DØ collaborations)

Duke University, Department of Physics, Box 90305, Durham NC 27708

ABSTRACT

With the advent of the Tevatron Run 2, the collider experiments, CDF and DØ, have reestablished the top quark and the W and Z signals and have begun programs of precision measurements of top quark and electroweak properties. We will survey some of the first Run 2 results from these analyses, and when appropriate compare with the Run 1 results. Finally we will give the status of Higgs boson searches and prospects at the Tevatron.

arXiv:hep-ex/0310057v1 29 Oct 2003

1 Introduction

After the success of the Fermilab Tevatron “Run 1” (1992 - 1995), operating with protons on antiprotons with a center of mass energy of $\sqrt{s} = 1.8$ TeV and a bunch spacing of $3.6 \mu\text{s}$, a shutdown ensued to upgrade the accelerator and the collider experiment detectors (CDF and DØ) for “Run 2”.

The integrated luminosity used for physics results from Run 1 was about 100 pb^{-1} , with typical instantaneous luminosities of $1.5 \times 10^{31} \text{ cm}^{-2} \text{ s}^{-1}$ (with the best instantaneous luminosity about double this). Physics quality data from Run 2 started to be accumulated in earnest in the beginning of 2002, at a higher energy of $\sqrt{s} = 1.96$ TeV, and operating with a bunch spacing of 396 ns. The integrated luminosity goal for Run 2 has been reduced due to difficulties with accelerator performance, however, the aim now is accumulate between 5 fb^{-1} and 9 fb^{-1} by late this decade, which might still allow the Tevatron sufficient sensitivity to discover the Standard Model (SM) Higgs boson (or a “SM-like” Higgs boson), but clearly now with a reduced chance. The current status of the Tevatron is given in more detail elsewhere in these proceedings [1].

The CDF and DØ detectors are designed for general purpose use, with a tracking system within a superconducting solenoid (1.4 T at CDF and 2 T at DØ), calorimetry, and a muon detection system. Both detectors underwent major upgrades for Run 2, which involved new detectors, extended coverage of existing detector systems, and new DAQ and trigger systems. The tracking system consists of a silicon system for the precise measurement of secondary vertices from b quark decays ($c\tau = 140 \mu\text{m}$ which results in B hadrons traveling on average about 3 mm before decaying); a central tracking system for the measurement of particle momentum and charge, which at CDF consists of wire chambers (COT) and a time of flight (TOF) detector (new in Run 2), and at DØ consists of a Fiber Tracker. One of the important upgrades for both experiments is the use of tracking information in the trigger system, especially the use of silicon information to trigger on displaced vertices, to give very high statistics b and c quark samples. Figure 1 shows parts of the DØ and CDF tracking detectors. Outside the magnetic solenoid lies the electromagnetic and hadronic calorimeters for the measurements of energy deposition. Electrons, photons, and jets, deposit almost all their energy in the calorimeters. Muons travel through the calorimeters depositing only a small fraction of their energy, and are detected by the muon chambers (gas chambers) which surround the calorimeters and steel absorbers.

In the following sections we will summarise a selection of past results using

the CDF and DØ detectors, and discuss what we expect in the next several years, concentrating on the physics involving the top quark, some electroweak measurements, and searches for Higgs bosons. The Run 1 results presented here come from about 100 pb^{-1} of integrated luminosity, and the current Run 2 results from between 30 pb^{-1} and 70 pb^{-1} .

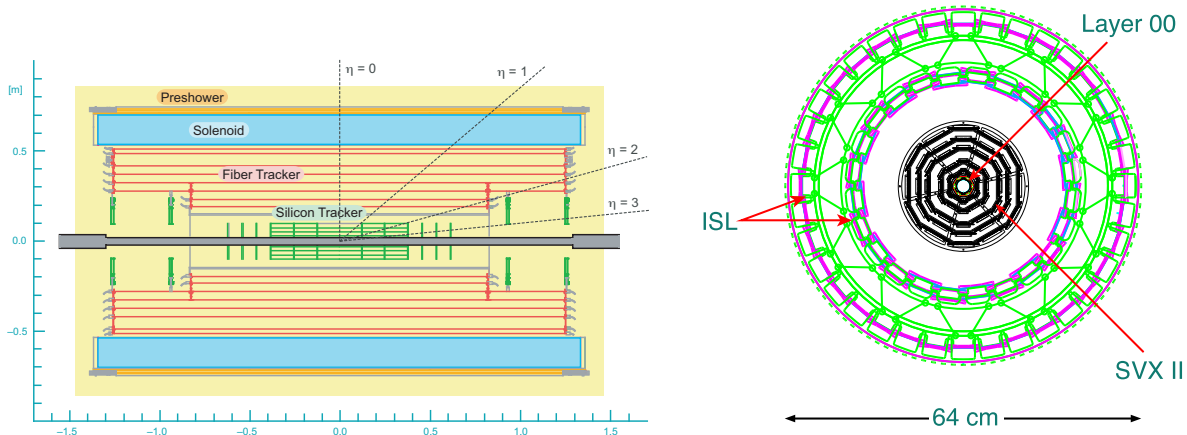


Figure 1: *The tracking system in Run 2 for DØ and CDF consists of silicon detectors within, a Fiber tracker for DØ, and a drift chamber for CDF. Shown here is a side view of the DØ tracking system (left) and a transverse view of the CDF silicon detectors.*

2 W and Z bosons

The large W and Z production cross-sections at the Tevatron (at $\sqrt{s} = 2 \text{ TeV}$; $\sigma(p\bar{p} \rightarrow W + X) \times B(W \rightarrow \ell\nu) \sim 2.7 \text{ nb}$, $\sigma(p\bar{p} \rightarrow Z + X) \times B(Z \rightarrow \ell^+\ell^-) \sim 0.26 \text{ nb}$) give large statistics data samples for precision measurements of vector boson properties. Only the leptonic decays are used, with the electron and muon channels providing the cleanest signals, but with the tau channels also considered to provide tests of lepton universality. The $W \rightarrow e\nu, \mu\nu$ and $Z \rightarrow e^+e^-, \mu^+\mu^-$ cross-section samples are also used extensively in other analyses for the determination of energy scales, resolutions, lepton identification efficiencies, and checks of detector responses and analysis tools.

The $W \rightarrow \ell\nu$ signature is large missing transverse energy (\cancel{E}_T , typically required to be $> 25 \text{ GeV}$) and a central isolated lepton with large transverse momentum (P_T). The backgrounds are roughly 10% for the electron and muon channels and 25% for the tau decay channel. The $Z \rightarrow \ell^+\ell^-$ signature is 2 central high- P_T leptons with opposite charge. The signal is very clean for the electron and muon

Table 1: *Summary of Tevatron Run 2 W and Z production cross-section measurements from data taken up until January 2003. The uncertainties given are statistical, systematic, and from the luminosity measurement, in that order.*

	DØ		CDF	
	# events	$\sigma \times B(W \rightarrow \ell\nu)$ (nb)	# events	$\sigma \times B(W \rightarrow \ell\nu)$ (nb)
e	27370	$3.05 \pm 0.10 \pm 0.09 \pm 0.31$	38625	$2.64 \pm 0.01 \pm 0.09 \pm 0.16$
μ	7352	$3.23 \pm 0.13 \pm 0.10 \pm 0.32$	21599	$2.64 \pm 0.02 \pm 0.12 \pm 0.16$
τ			2346	$2.62 \pm 0.07 \pm 0.21 \pm 0.16$
	# events	$\sigma \times B(Z \rightarrow \ell\ell)$ (pb)	# events	$\sigma \times B(Z \rightarrow \ell\ell)$ (pb)
e	1139	$294 \pm 11 \pm 8 \pm 29$	1830	$267 \pm 6 \pm 15 \pm 16$
μ	1585	$264 \pm 7 \pm 17 \pm 16$	1631	$246 \pm 6 \pm 12 \pm 15$

channels with backgrounds less than 1%. At the time of this presentation the tau decay channel analysis was still in progress.

The Run 2 status of the W and Z cross-section measurements is summarised in Table 1. Figure 2 shows the transverse mass spectra used for the $W \rightarrow \mu\nu$ cross-section and W width measurements. In Figure 3 the current Run 2 W and Z cross-section measurements are compared with the NNLO prediction [2].

In the near future both experiments will significantly improve the precision of these measurements, together with various other precision measurement not discussed here such as the W mass, W width, W charge asymmetry, W polarization, Drell-Yan mass and forward-backward asymmetry.

3 Diboson production

The cross-sections for heavy diboson production (WW , WZ , ZZ) are of the same order as for $t\bar{t}$ [3], but the signal is harder to discriminate over background processes. After enough data in Run 2 these cross-sections will be measured and used to set stringent limits on anomalous triple gauge boson couplings. The measurement and understanding of WW and WZ production will also serve as an important precursor for associated Higgs production searches ($q\bar{q} \rightarrow VH$ ($V = W, Z$)). In particular, WZ production with $Z \rightarrow b\bar{b}$ will provide a good calibration for associated production of light Higgs with $H \rightarrow b\bar{b}$. For heavier Higgs masses where the decay $H \rightarrow WW^*$ dominates, WW production will be the major background, and the Higgs searches will be natural extensions of these analyses. Both DØ and CDF have started studying WW production in Run 2 in the “dilepton” decay channel (with a handful of candidate events), from which both the WW production cross-section

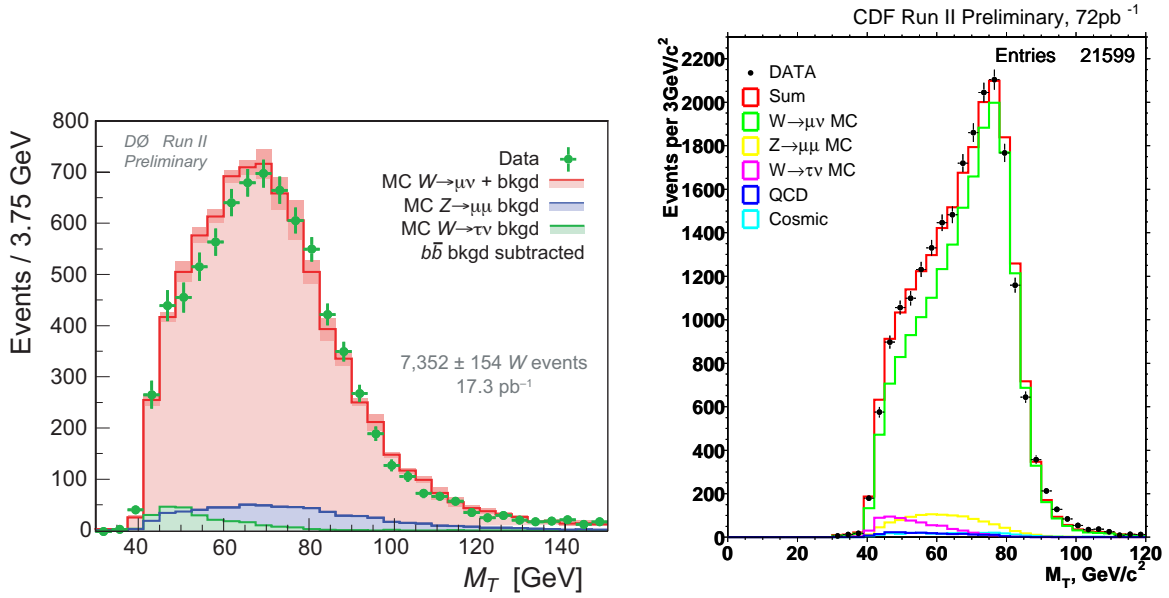


Figure 2: *Transverse mass distributions of $W \rightarrow \mu\nu$ candidates from $D\bar{O}$ (left) and CDF (right) from the Run 2 data used for the cross-section measurements in Table 1.*

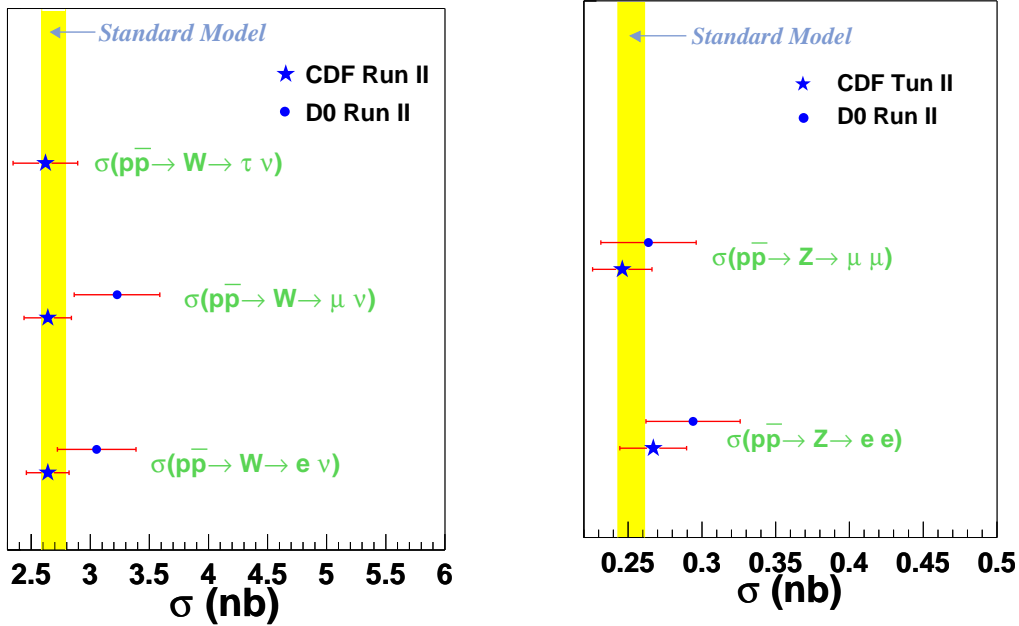


Figure 3: *Comparison of the Run 2 Tevatron W and Z cross-section measurements with NNLO calculations.*

measurement will come, in addition to limits on $H \rightarrow WW^*$ production.

4 Top quark physics

With Run 2 now well underway, top quark physics has moved from its discovery phase to precision measurements of top quark properties. With the top quark being such an unusual object with its very large mass it may be closely connected to new physics which precision measurements could help unveil. At the Tevatron top quarks are produced predominantly in pairs via the strong interaction, with a cross-section at $\sqrt{s} = 1.8 \text{ TeV}$ of about $\sigma_{t\bar{t}} = 5 \text{ pb}$, and at $\sqrt{s} = 2.0 \text{ TeV}$ about 7 pb [4]. The top quark can also be produced singly via the electroweak interaction with about half the $t\bar{t}$ cross-section, but with a final state that is much more difficult to extract from background processes. The observation of single top production is one of the main goals of the top physics program in Run 2. The top quark decays almost exclusively to Wb , and it is the different combinations of W decays that characterise the $t\bar{t}$ decay channels. The “dilepton” decay channel is that in which both W ’s decay leptonically and has a branching ratio of about 5% (we only consider W decays to $e\nu$ and $\mu\nu$ for now). In the “lepton + jets” decay channel one W decays leptonically and the other hadronically (the branching ratio is about 30%), and in the “all-hadronic” decay channel both W ’s decay hadronically (the branching ratio is about 45%).

The dilepton channel is therefore characterised by 2 highly energetic leptons (e or μ with $P_T > 20 \text{ GeV}$) from the W decays, a large amount of missing energy (\cancel{E}_T) from the W decay neutrinos, and 2 jets from the fragmentation of the 2 b quarks. The main backgrounds include Drell-Yan production of e^+e^- , $\mu^+\mu^-$ and $\tau^+\tau^-$ (where both taus decay to an electron or a muon), and WW production. The lepton + jets channel is characterised by one energetic lepton, large \cancel{E}_T , and 4 jets (from the 2 b quarks and the hadronic W decay). The dominant background is $W + jets$. Lastly, the all-hadronic channel is, as its name suggests, characterised by 6 jets only, where the dominant background is the QCD production of jets. Table 2 summarises the expected observations from top production at the Tevatron, and for comparison, at the LHC.

To increase the signal to background ratio in the lepton + jets and all-hadronic decay channels, extensive use is made of the silicon vertex (SVX) detectors, which can identify the secondary vertices from b quark decays. In Run 1 the CDF SVX detector provided an efficiency for identifying at least one of the b quarks from $t\bar{t}$ decay of about 50%.

In addition, when b quarks decay leptonically (branching ratio of about

Table 2: Summary of expected top production numbers at the Tevatron Run 1 and Run 2, and compared with the LHC. The expected observed numbers in the various decay channels (the last 4 rows) use expected efficiencies for observing top events.

	Run 1 (100 pb ⁻¹)	Run 2 (per fb ⁻¹)	LHC (per 10 fb ⁻¹)
CM Energy (TeV)	1.8	1.96	14.0
Peak Luminosity (cm ⁻² s ⁻¹)	2 × 10 ³¹	2 × 10 ³²	1 × 10 ³³
$\sigma(t\bar{t})$ (pb)	5.0	7.0	800
σ (single top)	2.5	3.4	320
Number of ($t\bar{t}$) produced	500	7000	8,000,000
Number of single top produced	250	3500	3,200,000
$N(t\bar{t} \rightarrow \ell^+\ell^- + \cancel{E}_T + 2 \text{ jets})$ (“dilepton”)	4	80	50,000
$N(t\bar{t} \rightarrow \ell + \geq 3j)$ (≥ 1 b -tag)	25	700	400,000
$N(t\bar{t} \rightarrow \ell + \geq 4j)$ (2 b -tags)	5	300	200,000
N (single t) ($W + 2 \text{ jets}$ with 1 b -tag)	3	70	60,000

20% for e or μ), one can “tag” the jet as coming from a b quark by identifying the lepton in the jet (hereafter called an SLT tag). This has a much lower efficiency due to the difficulty in identifying these leptons and the low branching ratio of b 's to leptons. For a $t\bar{t}$ event the efficiency of tagging at least one of the b jets in this way is about 20%. In Run 1 DØ did not have an SVX detector so made extensive use of this method of identifying b quarks, in addition to exploiting kinematic differences between $t\bar{t}$ and background processes, in order to increase the signal to background ratio.

In Run 2 both experiments have preliminary results from using b lifetime information provided by silicon tracking. The current b -tagging algorithms in both experiments are somewhat different but both have an efficiency to tag a $t\bar{t}$ event of roughly 50%, which will increase with more optimised algorithms in the near future.

In Run 1 measurements of top quark properties were limited by the low statistics available, and all errors were dominated by statistical uncertainties. The Run 1 measurements of the top mass and cross-sections in the various decay channels are summarised in Table 3. Details of the various analyses contributing to these results, and others, can be found in reference [5].

Preliminary Run 2 measurements of the $t\bar{t}$ production cross-section and mass have been made, which represents the beginning of a wealth of top physics

Table 3: *Summary of top quark properties as measured by the Tevatron from about 110 pb⁻¹ of data in Run 1. The measured cross-sections are shown for each decay channel of $t\bar{t}$ separately, and for the combination of channels. The top mass shown for each experiment is the result of combining the measurements in all decay channel.*

Property	CDF measurement	DØ measurement	CDF + DØ
Mass (GeV/ c^2)	176.1 ± 6.6	172.1 ± 6.8	174.3 ± 5.1
$\sigma_{t\bar{t}}$ (dilepton) (pb)	$8.4^{+4.5}_{-3.5}$	6.4 ± 3.4	
$\sigma_{t\bar{t}}$ (lepton + jets) (pb)	$5.7^{+1.9}_{-1.5}$	5.2 ± 1.8	
$\sigma_{t\bar{t}}$ (all-hadronic) (pb)	$7.6^{+3.5}_{-2.7}$	7.1 ± 3.2	
$\sigma_{t\bar{t}}$ (combined) (pb)	$6.5^{+1.7}_{-1.4}$	5.9 ± 1.7	

measurements at the Tevatron in the next few years. As the precision of the top quark measurements increases in the coming years at the Tevatron, any possible new physics associated with the top quark could well be uncovered.

Tables 4 and 5 summarise the first Run 2 $t\bar{t}$ cross-section measurements at $\sqrt{s} = 1.96$ TeV from the Tevatron experiments. The lepton + jets results shown in Table 5 are those that require at least one jet in the event be tagged using silicon information. Both CDF and DØ employ an algorithm which reconstructs the secondary vertex using tracks from the b decay and places a requirement on the measured distance from the primary vertex (called an SVX tag at CDF and an SVT tag at DØ). In addition DØ has results using a different algorithm which requires at least 2 tracks in the jet with a significant impact parameter (the perpendicular distance in the transverse plane from the track to the primary vertex). This is called a “CSIP” tag.

In addition to the lepton + jets results shown in Table 5 DØ also has a preliminary combined measurement using similar topological and SLT analyses as were used in Run 1 ($W + \geq 3$ events with either a fourth jet or one of the 3 jets with a soft lepton tag, plus some additional kinematic requirements). The preliminary result of combining the topological and SLT lepton + jets analyses in about 45 pb⁻¹ of Run 2 data is:

$$\sigma_{t\bar{t}} = 8.5^{+4.5}_{-3.6}(\text{stat})^{+6.3}_{-3.5}(\text{syst})^{+0.8}_{-0.8}(\text{lum}) \text{ pb}$$

The Run 2 CDF $t\bar{t}$ dilepton candidates are shown in Figure 4 and compared with the Run 1 results. After 2 fb⁻¹ of Run 2 data both experiments expect about 150 dilepton candidates, providing a beautiful sample of events in which to look for deviations from SM expectations (expected signal to background better than 5:1 for optimised analyses).

As Run 2 progresses the statistical limitations of the results presented

Table 4: Preliminary Run 2 $t\bar{t}$ production cross-section measurements from $D\emptyset$ and CDF in the dilepton channel. The Run 2 integrated luminosity for these measurements is 72 pb^{-1} for CDF, and for $D\emptyset$ 48 pb^{-1} for ee , 33 pb^{-1} for $\mu\mu$, and 42 pb^{-1} for $e\mu$.

$D\emptyset$	ee	$\mu\mu$	$e\mu$
Background	1.00 ± 0.48	0.59 ± 0.30	0.07 ± 0.01
Expected $t\bar{t}$	0.25 ± 0.02	0.30 ± 0.02	0.50 ± 0.01
Run 2 data	4	2	1
$\sigma_{t\bar{t}}$ (pb)	$29.9^{+21.0}_{-15.7}(\text{stat})^{+14.1}_{-6.1}(\text{syst})^{+3.0}_{-3.0}(\text{lum})$		
CDF	ee	$\mu\mu$	$e\mu$
Background	0.10 ± 0.06	0.09 ± 0.05	0.10 ± 0.04
Expected $t\bar{t}$	0.47 ± 0.05	0.59 ± 0.07	1.44 ± 0.16
Run 2 data	1	1	3
$\sigma_{t\bar{t}}$ (pb)	$13.2^{+7.3}_{-5.4}(\text{stat})^{+2.0}_{-0.8}(\text{syst})^{+0.8}_{-0.8}(\text{lum})$		

Table 5: Preliminary Run 2 $t\bar{t}$ production cross-section measurements from $D\emptyset$ and CDF in the lepton + jets channel where at least one jet is required to be tagged by the SVX. Results are shown from $D\emptyset$ using 2 different secondary vertex tagging algorithms. The Run 2 integrated luminosity for these measurements is 58 pb^{-1} for CDF, and for $D\emptyset$ about 45 pb^{-1} . The 3 and ≥ 4 jet events are used for the cross-section measurements.

$D\emptyset$ (CSIP)	$W + 1$ jet	$W + 2$ jets	$W + 3$ jets	$W + \geq 4$ jets
Background	30.6 ± 5.0	26.4 ± 3.5	8.3 ± 1.3	2.5 ± 0.7
SM Background + $t\bar{t}$	30.6 ± 5.0	27.1 ± 3.6	11.1 ± 1.4	6.5 ± 1.0
Run 2 data	34	27	13	6
$\sigma_{t\bar{t}}$ (pb)	$7.4^{+4.4}_{-3.6}(\text{stat})^{+2.1}_{-1.8}(\text{syst})^{+0.7}_{-0.7}(\text{lum})$			
$D\emptyset$ (SVT)	$W + 1$ jet	$W + 2$ jets	$W + 3$ jets	$W + \geq 4$ jets
Background	27.0 ± 5.0	24.0 ± 4.0	7.5 ± 1.5	2.3 ± 0.6
SM Background + $t\bar{t}$	27.0 ± 5.0	24.6 ± 4.1	10.1 ± 1.6	6.0 ± 0.9
Run 2 data	28	20	9	9
$\sigma_{t\bar{t}}$ (pb)	$10.8^{+4.9}_{-4.0}(\text{stat})^{+2.1}_{-2.0}(\text{syst})^{+1.1}_{-1.1}(\text{lum})$			
CDF (SVX)	$W + 1$ jet	$W + 2$ jets	$W + 3$ jets	$W + \geq 4$ jets
Background	33.8 ± 5.0	16.4 ± 2.4	2.9 ± 0.5	0.9 ± 0.2
SM Background + $t\bar{t}$	34.0 ± 5.0	18.7 ± 2.4	7.4 ± 1.4	7.6 ± 2.0
Run 2 data	31	26	7	8
$\sigma_{t\bar{t}}$ (pb)	$5.3^{+2.1}_{-1.8}(\text{stat})^{+1.3}_{-0.6}(\text{syst})^{+0.3}_{-0.3}(\text{lum})$			

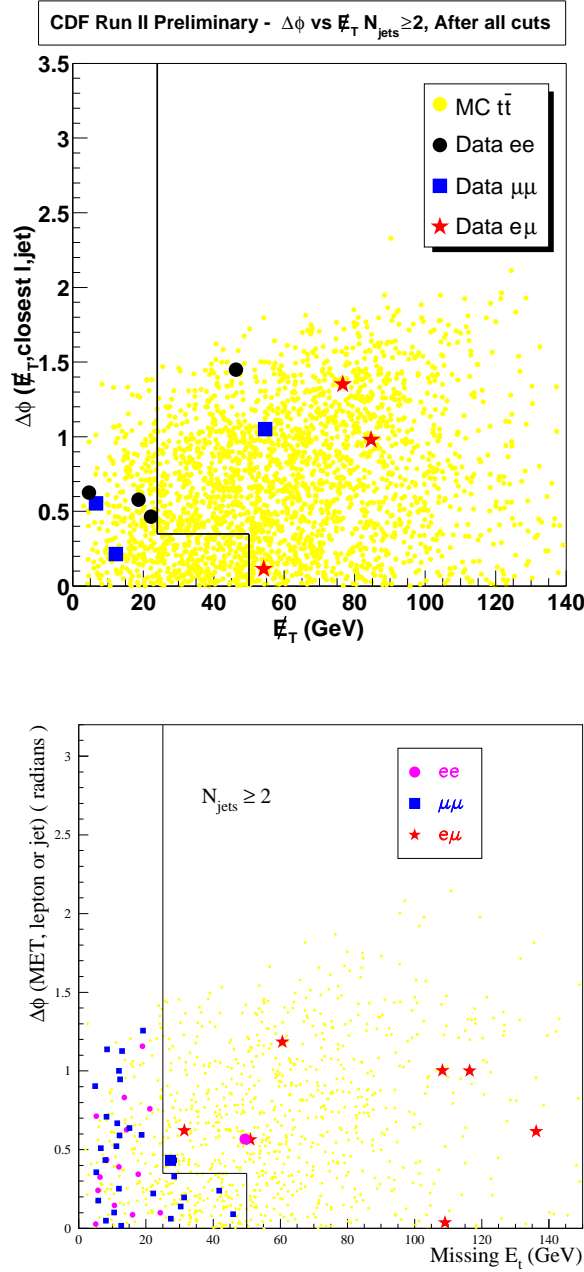


Figure 4: The CDF $t\bar{t}$ dilepton + ≥ 2 jet events in the $\Delta\phi$ versus E_T plane, for both Run 1 (bottom) and the first 72 pb^{-1} of Run 2 (top), where $\Delta\phi$ is the azimuthal angle between the E_T and the nearest lepton or jet in the event. The “L” indicates the E_T and $\Delta\phi$ requirements in the analysis. The Run 2 analysis has an additional cut on the total energy in the event, without which there is an addition 2 candidates (and so is a fairer comparison to the Run 1 results). In the Run 1 analysis 9 candidates were observed with a background estimate of 2.4 ± 0.5 events and an expected $t\bar{t}$ contribution of 3.9 events.

here will be reduced dramatically, and after a few hundred pb^{-1} of data the main limitations will be systematic. At the time of this writing new cross-section measurements are about to come out using more than 100pb^{-1} , and this continual improvement of top quark measurements will continue for the next several years. The top cross-section measurements from Run 1, together with the first Run 2 results are summarised in Figure 5. The Run 2 results shown are only the combined $D\bar{O}$ topological and SLT cross-section given above, and the combination of the CDF lepton + jets and dilepton cross-sections, which gives a result of $\sigma_{t\bar{t}} = 6.9_{-2.0}^{+2.5} \text{pb}$. Shown for comparison is a NLO prediction [4] where the upper and lower curves represent doubling and halving the central scale of m_{top} and incorporate the spread from different PDF's.

Run 2 measurements of the top mass in both the dilepton and lepton + jets channels are also in progress. After accumulating approximately 1fb^{-1} of Run 2 data, it is expected the $t\bar{t}$ production cross-section will be measured to about 10%, and the top mass to about 3 GeV. In both cases combinations of $D\bar{O}$ and CDF analyses are planned to improve the overall Tevatron sensitivity.

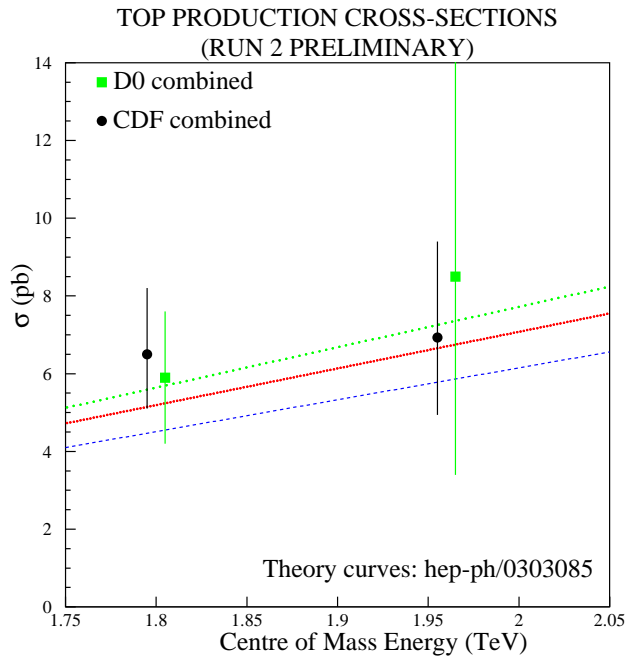


Figure 5: *Summary of the $D\bar{O}$ and CDF Run 1 $t\bar{t}$ production cross-section measurements at $\sqrt{s} = 1.8 \text{ TeV}$, together with the first Run 2 results, as compared with a NLO calculation.*

5 Searches for the Higgs

Within the SM mass is generated, and the electroweak symmetry is broken, by the Higgs mechanism. All the particles of the SM have been observed, except for the Higgs boson, so its discovery is currently one of the most important goals in high energy physics. Precision electroweak measurements (including the top mass) predict a light SM Higgs [6] of $88_{-35}^{+53} \text{ GeV}/c^2$. The expected light Higgs makes it possible to discover at the Tevatron in the next few years, although with the reduced predicted Run 2 integrated luminosity this goal is now less likely. In Run 1 CDF and DØ conducted searches for low mass Higgs bosons ($M_H < 120 \text{ GeV}/c^2$), using its associated production with vector bosons (W^\pm or Z^0). At such masses the Higgs decays predominantly to $b\bar{b}$. Therefore, even though the cross-section for $gg \rightarrow H$ (0.7 pb at $M_H = 120 \text{ GeV}/c^2$) is much larger than the cross-sections for WH and ZH production (0.16 pb and 0.10 pb respectively at $M_H = 120 \text{ GeV}/c^2$ and $\sqrt{s} = 2 \text{ TeV}$) [7], the Tevatron experiments are more sensitive to the latter production mechanisms, as single Higgs production is overwhelmed by an irreducible QCD di-jet background.

In Run 1 searches were conducted in the following associated SM Higgs decay channels:

- $ZH \rightarrow \ell\ell b\bar{b}$ (with at least 1 b -tagged jet): signal characterised by 2 highly energetic leptons ($P_T > 20 \text{ GeV}$) and 2 jets.
- $ZH \rightarrow \nu\nu b\bar{b}$ (with at least one b -tagged jet): signal characterised by large missing energy and 2 jets.
- $WH \rightarrow \ell\nu b\bar{b}$ (with at least one b -tagged jet): signal characterised by one energetic lepton, large missing energy and 2 jets.
- $W/ZH \rightarrow qq' b\bar{b}$ (with at least two b -tagged jets): signal characterised by 4 jets.

In the absence of any observed signal, cross-section limits were determined by fitting the observed spectra to a combination of the expected di-jet spectra from background processes and from WH and ZH signal. Figure 6 summarises the CDF 95% confidence level (CL) cross-section limits for all the individual decay channels as well as the combined result, as a function of the Higgs mass. The limits are about 30 times higher than the SM predictions, which sets the scale for the luminosity needed in order to observe the SM Higgs boson in Run 2.

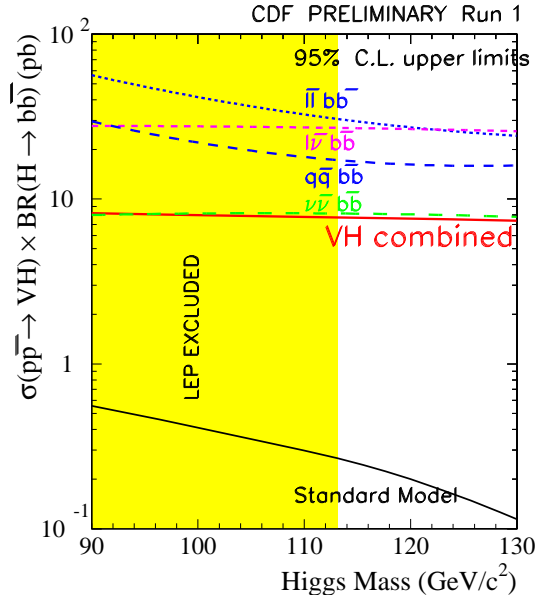


Figure 6: *CDF Run 1 results from searches for the SM Higgs boson. The 95% confidence level limits for $WH + ZH$ production are shown as a function of Higgs mass for the different decay channels analysed. Also shown is the region excluded by LEP2.*

In Run 2 b -tagging and the resolution of the $b\bar{b}$ invariant mass is critical for light Higgs searches. To this end, the success of the CDF and DØ silicon vertex triggers is crucial, from which a large $Z \rightarrow b\bar{b}$ sample will be obtained for calibrating the tagging efficiency and mass resolution. It is also important for CDF and DØ to combine results for maximal sensitivity. Run 2 sensitivity studies indicate that with about 10 fb^{-1} of data (the current upper limit projected for Run 2) evidence for Higgs production at the 3σ level is possible for $M_H < 130 \text{ GeV}/c^2$, and exclusion at the 95% level is possible up to a Higgs mass of $180 \text{ GeV}/c^2$ [8]. In Run 2 searches for $H \rightarrow W^+W^-$ are also in progress which will provide limits in the intermediate Higgs mass range (assuming something isn't found).

6 Conclusions

Both the CDF and DØ detectors are working well in Run 2 and the understanding of their performance is now leading to high quality physics results. We have reported on preliminary Run 2 results in electroweak and top quark physics, and summarised the relevant Run 1 results for comparison. With the recent improvements in the Tevatron's performance, these Run 2 results represent the beginning of

a rich program in electroweak, top quark, and Higgs physics in the next few years.

7 Acknowledgements

I would like to thank the organisers of the PIC 2003 conference for a stimulating and well organised series of presentations. This work was supported by the U.S. Department of Energy and National Science Foundation; the Italian Istituto Nazionale di Fisica Nucleare; the Ministry of Education, Science and Culture of Japan; the Natural Sciences and Engineering Research Council of Canada; the National Science Council of the Republic of China; and the A.P. Sloan Foundation.

References

1. F. Azfar, *these proceedings*.
2. A. D. Martin *et al.*, Phys. Lett. B **531**, 216 (2002).
3. J. M. Campbell, R. K. Ellis, hep-ph/9905386.
4. M. Cacciari, S. Frixione, M. L. Mangano, P. Nason, G. Ridolfi, hep-ph/0303085.
5. D. Chakraborty, J. Konigsberg, D. Rainwater, Submitted to Ann. Rev. Nucl. Part. Sci., hep-ph/0303092, and references therein.
6. The LEP electroweak working group: <http://lepewwg.web.cern.ch/LEPEWWG/>
7. M. Spira, hep-ph/9810289.
8. M. Carena, J. Conway, H. Haber, J. Hobbs *et al.*, Report of the Tevatron Higgs Working Group, hep-ph/0010338.